Reactions $\bar{p}p \to p\pi^{\pm}X$ and a comparison with leptoproduction and the quark-parton model

M. Pratap, R. Lewis, B. Y. Oh, G. A. Smith, and J. Whitmore
Department of Physics, Michigan State University, East Lansing, Michigan 48824

R. E. Ansorge, C. Booth, P. Elcombe, J. R. Carter, W. W. Neale, J. G. Rushbrooke, A. Simmons, D. R. Ward, and T. O. White
Cavendish Laboratory, Cambridge, England

(Received 21 August 1978)

We have studied the inclusive reactions $\bar{p}p \to p\pi^{\pm}X$ at 8.9 GeV/c and compared them to the lepton-induced processes $e^-p \to e^-\pi^{\pm}X$ and the photoproduction reactions $\gamma p \to \pi^{\pm}X$. The naive quark-parton model is found to be quite successful in interpreting the results. The distribution of charge in the current-fragmentation region is consistent with production of $\pi^{\pm}$ via absorption of the current by fractionally charged valence antiquarks of the antiproton.

INTRODUCTION

Using data obtained from the SLAC hybrid facility, we have studied some features of the inclusive reactions $\bar{p}p \to p\pi^{\pm}X$ at 8.9 GeV/c and compared them to those observed in the lepton-induced processes $e^-p \to e^-\pi^{\pm}X$ and in the photoproduction reactions $\gamma p \to \pi^{\pm}X$. Such a comparison may help clarify the long-standing proposal that the coupling of the Pomeron to hadrons should be like that of the photon.[1] A relationship between hadron- and lepton-induced reactions is also expected in terms of quark-parton dynamics if an underlying field theory such as quantum chromodynamics is correct. In fact the quark-parton model has recently been shown to give an excellent description of inclusive hadronic reactions in the fragmentation region.[2] Brodsky and Gunion, on the other hand, have studied jet production as a link between hadron- and lepton-induced reactions.[3]

APPARATUS

The apparatus used in this experiment consists of the SLAC Hybrid Facility[4] with the 40-in. hydrogen-filled bubble chamber operating at 10 expansions/sec, an upstream beam Čerenkov counter, upstream and downstream proportional wire chambers (PWC), a downstream Čerenkov counter (CANUTE), and a neutral-particle calorimeter. The beam Čerenkov counter is a 1.5-m Freon counter operated at 1 atmosphere with both K's and p's being below threshold. The two upstream PWC's have an active area of 8 in. × 8 in. with a 2-mm wire spacing while the three downstream PWC's have active areas ranging from ~20 cm × 60 cm to ~30 cm × 1 m with 2-mm wire spacing. CANUTE is a large ten-celled Freon-12 high-pressure [59 psi (absolute)] Čerenkov counter with a 10-GeV/c proton threshold. The calorimeter consists of 28 scintillation counters interspersed among 2 lead and 26 iron plates of approximately 30 × 30 in.^{2} cross section. In addition three sets of 5 × 5 hodoscope counters are utilized to help separate charged-hadron interactions or γ-ray showers from antineutron interactions.

The 8.9-GeV/c beam was run at an intensity of about one $\bar{p}$/beam pulse, requiring a primary electron beam current of about 8 mA. A beam contamination of 0.8 light particles/$\bar{p}$ was reduced to a few percent by the beam Čerenkov counter. Approximately 1% of the heavy particles are K^- and have been ignored in this analysis.

The bubble chamber was exposed to 3×10^5 pictures with the $\bar{p}$ beam and 1.5×10^5 pictures with a proton beam at 8.9 GeV/c momentum. The bulk of the data was taken in a triggered mode with a software trigger designed to ensure that a $\bar{p}$ (or p) beam track had entered the bubble chamber and had undergone an interaction (deflection) within a preselected fiducial volume of the bubble chamber. About 50% of the pictures have a good event with the interaction vertex calculated on line, together with all the electronics information available.

DATA

For this study we have used all events which contain a proton (with momentum less than 1.4 GeV/c) identified by ionization in the bubble chamber. We estimate that we have identified $\gtrsim 70\%$ of the cross section for the process

$$\bar{p}p \to pX \text{ at } 8.9 \text{ GeV}/c\,. \tag{1}$$

Having selected these events from a sample of ~10 000 inclusive $\bar{p}p$ events, we study the two-particle inclusive reactions

 © 1979 The American Physical Society

$$\bar{p}p \to p\pi^{\pm}X. \quad (2)$$

The identification of the second positive particle as a π^+ is unambiguous since we have already identified a proton in each event. To distinguish between $\bar{p}$ and π^- we have used CANUTE. However, owing to δ rays and accidentals in CANUTE and the probability for a $\bar{p}$ to interact somewhere between the bubble-chamber vertex and the Čerenkov hodoscope, the efficiency for $\bar{p}$ identification in CANUTE is reduced to about 75%. We estimate therefore that $\lesssim$15% of the negative tracks that have been called π^- in reaction (2) are misidentified $\bar{p}$'s. In the following, we will be considering $\pi^{\pm}$ production in the forward hemisphere of the exchanged-particle–beam-particle rest system (forward with respect to the exchanged particle). In this region of phase space there are only a few $\bar{p}$'s and utilizing the measured distribution of identified $\bar{p}$'s we estimate that no more than 4% of the tracks labeled π^- in the forward hemisphere are in fact misidentified $\bar{p}$'s. For the small sample of π^- which enter CANUTE, the decision between π^- and $\bar{p}$ has been made based on the downstream electronic information.

Reaction (2) can be thought of as proceeding via an exchange mechanism [see Fig. 1(a)], "Γ" $\bar{p} \to \pi^{\pm}X$, in analogy with the electromagnetic or weak processes. To start with, "Γ" is a fictitious mathematical entity, with its momentum and energy defined by the target and the recoil protons. We will try to give "Γ" a definite physical meaning by comparing the above reaction to the process $e^-p \to e^-\pi^{\pm}X$ in which the virtual photons probe the underlying structure of the proton [Fig. 1(b)]. For small $W^2 \equiv (p_1+p_2-p_3)^2$ and small $Q^2 = (p_1-p_3)^2$ (where p_1, p_2, p_3 are the four-momenta of the target, beam, and recoil proton, respectively) the process "Γ" $\bar{p} \to \pi^{\pm}X$ will be shown to bear a remarkable similarity to the virtual-photon reaction "γ" $p \to \pi^{\mp}X$ and to the corresponding photoproduction reaction. This comparison indicates that the hadronic current "Γ" couples to hadrons in a way similar to that of a virtual photon and, in particular, "Γ" interacts individually with the quark partons of the $\bar{p}$ to produce hadrons (for small W^2 and small Q^2).

In Fig. 2(a) we show the missing mass squared (W^2) recoiling against the proton for inelastic events. The center-of-mass energy available for the reaction is $\sqrt{s} \approx 4.2$ GeV. We will divide the data into two sets: $W < 2$ GeV and $W > 2$ GeV, respectively. The $\bar{p}$ fragmentation is expected to dominate in the former and that is where we expect to find the "Γ" $\leftrightarrow \gamma$ analogy to be most successful. The distribution of momentum transfer squared (Q^2) imparted to the proton for inelastic events [shown in Fig. 2(b)] is observed to be

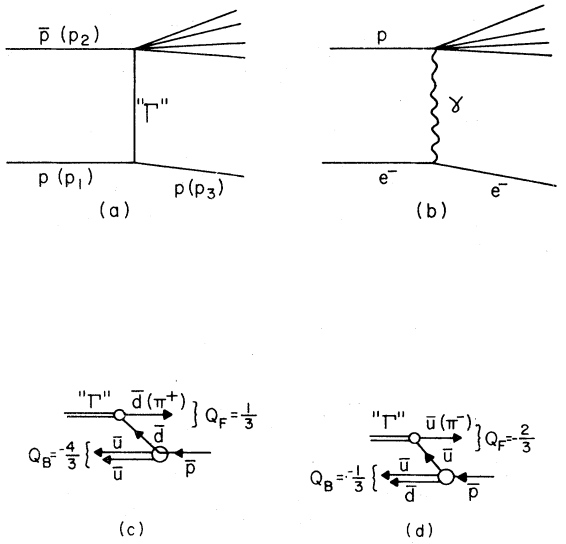

FIG. 1. (a) A particular mechanism for the reaction $\bar{p}p \to p + X$. (b) One-photon-exchange diagram for $e^-p \to e^-X$. (c) Production of π^+ and (d) π^- via absorption of a current by the valence antiquarks of the antiproton.

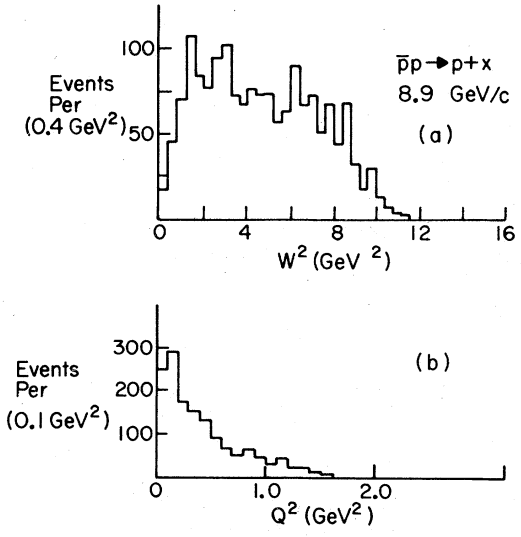

FIG. 2. (a) Missing mass squared recoiling against the proton. (b) Momentum transfer squared imparted to the recoil proton.

highly peripheral. Almost all the data have $Q^2 < 1.0$ GeV^2. We now transform all physical variables to the center of mass of the process "Γ"$\bar{p} \to \pi^\pm X$, where the four-momentum of "Γ" is given by $p_\Gamma = p_1 - p_3$. In this frame, the invariant Feynman-x distribution of the π^+ is shown in Fig. 3(a) for $W < 2$ GeV. Here we define $x = 2P_L^*/W$ where P_L^* is the momentum of the $\pi^\pm$ along the direction of "Γ" in the $\Gamma\bar{p}$ center of mass. W, the missing mass recoiling against the proton, is also the energy available for particle production in this frame.

The left-right asymmetry of the x distribution in Fig. 3(a) is noteworthy. There are more π^+ forward than in the backward direction. For comparison we have also shown the distribution for the electroproduction reaction $e^-p \to e^-\pi^-X$ for $1.8 < W < 2.2$ GeV and $0.3 < Q^2 < 1.4$ GeV^2 (Ref. 5) (dotted line). This distribution is observed to be not very sensitive with respect to W and Q^2. Data for the photoproduction reaction $\gamma p \to \pi^-X$ at $W = 2.8$ GeV (Ref. 6) are shown as a solid line.[7] For clarity we have ignored the errors (±10%) in the electroproduction and photoproduction data and have presented them by smooth curves. In addition, the distributions have been normalized by their respective total cross sections. The three different sets of data are fairly consistent with each other, especially in the backward direction ($x < 0$).

In contrast, the π^+ distribution for $W > 2$ GeV [Fig. 3(b)] shows somewhat different characteristics. It is, for example, even more asymmetric, and extends over a smaller range in x for both forward and backward regions. The cross section increases monotonically with x from $x = -0.6$ to $x = +0.6$ and then sharply drops to zero. These data bear less resemblance to the electroproduction and photoproduction data. The data for $\Gamma\bar{p} \to \pi^-X$ exhibit similar features (not shown).

We now compare the ratio for π^-/π^+ observed in the forward direction ($x > 0$) in the $\Gamma\bar{p}$ center-of-mass frame to the ratio π^+/π^- observed in the electroproduction process as a function of W, Q^2, and $1/\omega = Q^2/2M\nu$ where $\nu = p_2 \cdot Q/M$, M being the mass of the proton. [The electroproduction data[8] used here involve several "cuts," i.e., $\pi^\pm$'s are limited to $p_T^2 < 0.02$ (GeV/c)^2 and x is restricted to the region $0.4 < x < 0.7$. However, the data[8] show no strong dependence on either x or $p_T^2 < 0.2$ (GeV/c)^2 and so for this comparison we have not imposed these limits on our data.] Figures 4(a), 4(b), and 4(c) show the behavior of the ratio π^-/π^+ for our data and the ratio π^+/π^- for the electroproduction data as a function of W, $1/\omega$, and Q^2, respectively. We note that the ratio falls monotonically with increasing W, is constant with Q^2, and rises monotonically as a function of $Q^2/2M\nu$ within the small range of variables studied here. Again it is clear from Fig. 4 that both the

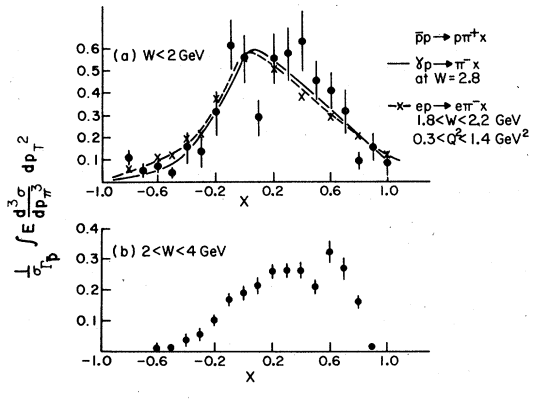

FIG. 3. (a) Invariant x distribution for π^+ in the reaction $\bar{p}p \to p\pi^+X$ in $\Gamma\bar{p}$ center-of-mass frame for $W < 2$ GeV. The dotted curve represents electroproduction data for $1.8 < W < 2.2$ GeV and $0.3 < Q^2 < 1.4$ GeV^2. The solid curve shows photoproduction data for $W = 2.8$ GeV. (b) Invariant x distribution for π^+ for $W > 2$ GeV.

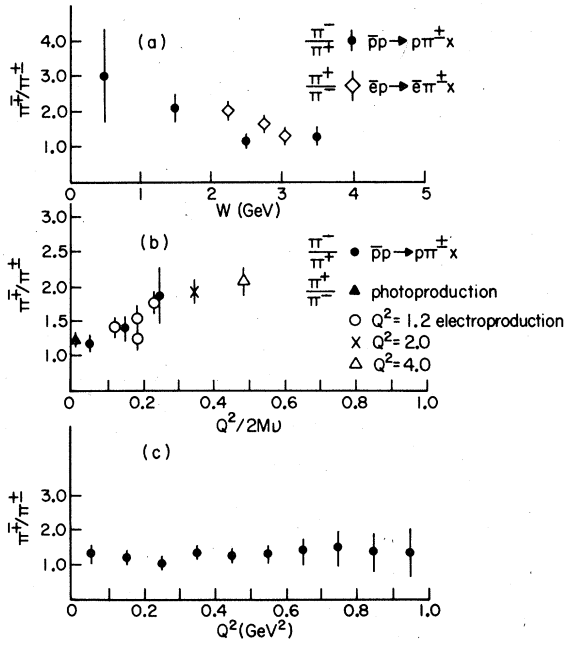

FIG. 4. The ratio π^-/π^+ for our data and the ratio π^+/π^- for electroproduction and photoproduction as a function of (a) W, (b) $1/\omega = Q^2/2M\nu$, and (c) Q^2.

behavior and the magnitude of this ratio as a function of these parton-model-motivated variables is remarkably similar in the hadron- and the lepton-induced reactions. We now make a further comparison with the quark-parton model.

The invariant x distribution for π^+ [Fig. 3(a)] follows closely the quark distribution[2] $x\bar{d}(x)$ in the backward direction ($\bar{p}$ fragmentation region). In fact, $x\bar{d}(x)$ is found to be practically the same as the solid line in the figure. In the following we take this coincidence seriously and interpret it to mean that "Γ" interacts incoherently with the antiquark partons of the $\bar{p}$ to produce π's. This interpretation gives rise to some interesting predictions[3] which can be tested with our data. In particular let us consider Figs. 1(c) and 1(d) which show respectively the production of a π^+ and a π^- in the forward hemisphere (current-fragmentation region) through the absorption of the current momentum by a $\bar{d}$ or a $\bar{u}$. On the basis of this model, if a π^+ is detected in the forward hemisphere in the $\Gamma\bar{p}$ center of mass, the mechanism of Fig. 1(c) is expected to dominate and the ratio of the charges in the forward and backward hemispheres is given by $Q_F/Q_B = +\frac{1}{3}/(-\frac{4}{3}) = -0.25$. On the other hand, if a π^- is detected in the forward direction, we predict, according to Fig. 1(d), $Q_F/Q_B = -\frac{2}{3}/(-\frac{1}{3}) = 2.0$. The corresponding experimental numbers determined from our data are as follows:

$$\left(\frac{Q_F}{Q_B}\right)_{\pi^+\text{ forward}} = -0.25 \pm 0.02$$

and

$$\left(\frac{Q_F}{Q_B}\right)_{\pi^-\text{ forward}} = 1.80 \pm 0.15,$$

in excellent agreement with the predictions made above.[9] It is interesting to note that these charge ratios can only be obtained with $\frac{1}{3}$ integral charges since $Q_F + Q_B = -1$. In pursuing this idea further, we have studied the correlation of the charge distribution in the $\Gamma\bar{p}$ center-of-mass frame with respect to the current direction. Let Q_F be the total charge in the hemisphere of the fastest $\pi^\pm$ (trigger) in the event and let θ be the angle between the trigger and current directions. Figure 5 shows the variation of Q_F as a function of $\cos\theta$ for π^+ and π^- triggers. It is remarkable that in the direction of the current ($\cos\theta = +1$) Q_F approaches $\frac{1}{3}$ and $-\frac{2}{3}$, respectively, as expected from Figs. 1(c) and 1(d). It is of interest to investigate whether these ratios are dependent on the quantum numbers of the trigger particle or only on its charge. We have thus selected events of the type

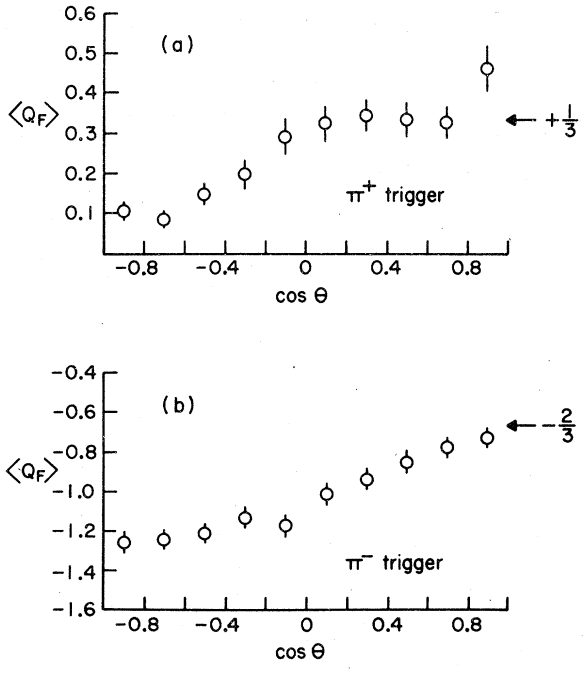

FIG. 5. Total charge in the hemisphere of (a) the π^+ trigger and (b) the π^- trigger as a function of the angle between the trigger and the current directions.

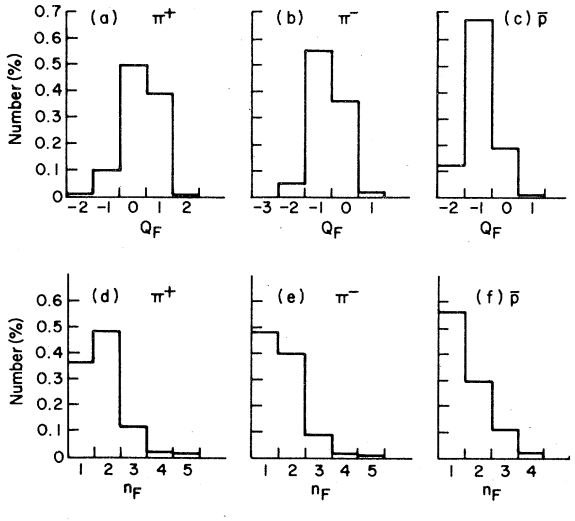

FIG. 6. Charge distributions in the forward hemisphere for (a) π^+, (b) π^- and (c) $\bar{p}$ triggers. The forward–hemisphere charged–particle multiplicities for (d), π^+, (e) π^-, and (f) $\bar{p}$ triggers.

$$\bar{p}p \to p\bar{p}X \quad (3)$$

and find that when we trigger on a forward (in the $\Gamma\bar{p}$ rest system) $\bar{p}$, the ratio

$$\left(\frac{Q_F}{Q_B}\right)_{\bar{p}\text{ forward}} = 9.0 \pm 1.5\,,$$

substantially different from the value quoted above for the π^- trigger. To investigate this in more detail, in Figs. 6(a) and 6(b) we show the charge distributions in the forward hemisphere for the π^+ and π^- triggers, respectively. Figures 6(d) and 6(e) show the number of particles in the forward hemisphere (including the trigger) for the π^+ and π^- triggers, respectively. These may be compared with the analogous distributions associated with a trigger $\bar{p}$ shown in Figs. 6(c) and 6(f). It is clear that the distributions for π^- and $\bar{p}$ triggers are quite different, indicating that more than just the charge quantum number of the trigger is important.

In conclusion, the reactions $\bar{p}p \to p\pi^{\pm}X$ have remarkable similarities to the lepton-induced reactions $e^-p \to e^-\pi^{\pm}X$. The naive interpretation of the data in terms of the underlying quark structure of the hadrons is quite successful.

ACKNOWLEDGMENTS

We would like to thank SLAC and SHF personnel and the scanning and measuring staffs at the two laboratories for their outstanding efforts. It is a pleasure to acknowledge informative discussions with N. Weiss and E. Lehman. This research was supported in part by the U. S. National Science Foundation and by the Science Research Council (U. K.).

---

[1]T. T. Chou and C. N. Yang, Phys. Rev. 175, 1832 (1968).

[2]K. P. Das and R. C. Hwa, Phys. Lett. 68B, 459 (1977); E. Lehman *et al.*, Phys. Rev. D 18, 3353 (1978).

[3]G. R. Farrar and J. L. Rosner, Phys. Rev. D 7, 2747 (1973); S. J. Brodsky and J. F. Gunion, in *Proceedings of the Seventh International Colloquium on Multiparticle Reactions, Tutzing/Munich, Germany, 1976*, edited by J. Benecke *et al.* (Max-Planck-Institut für Physik und Astrophysik, Munich, 1976), p. 369; S. J. Brodsky and N. Weiss, Phys. Rev. D 16, 2325 (1977).

[4]J. Ballam and R. Watt, Annu. Rev. Nucl. Sci. 27, 75 (1977).

[5]C. K. Chen *et al.*, Nucl. Phys. B133, 13 (1978).

[6]K. C. Moffeit *et al.*, Phys. Rev. D 5, 1603 (1971).

[7]J. P. DeBrion *et al.*, Phys. Lett. 52B, 477 (1974), have also compared 102-GeV/c $pp \to p\pi^-X$ data with the photoproduction data.

[8]C. J. Bebek *et al.*, Phys. Rev. D 15, 3085 (1977).

[9]The agreement between the naive quark-parton model and our results shows that the average quark charge retention $\langle \eta_c \rangle$ is small. Taking account of η_c (Ref. 3). one finds $\langle Q_F \rangle_{\pi^+} = +\frac{1}{3} + \langle \eta_c \rangle$ and $\langle Q_F \rangle_{\pi^-} = -\frac{2}{3} + \langle \eta_c \rangle$. In a specific model (see Ref. 3) with an SU(2)-symmetric sea this yields $\langle \eta_c \rangle = \frac{1}{6}$ and $\langle Q_F \rangle = \pm\frac{1}{2}$ for the $\pi^{\pm}$ triggers, whereas for an SU(3)-symmetric sea $\langle \eta \rangle = 0$ in agreement with our results.